Acta Cryst. (1980). A**36**, 803–808

Electron-Density Studies of Metal–Metal Bonds. I. The Deformation Density of Ti_2O_3 at 295 K

BY M. G. VINCENT,* K. YVON AND A. GRÜTTNER†

Laboratoire de Cristallographie aux Rayons X, Université de Genève, 24, Quai Ernest Ansermet, CH-1211 Genève 4, Switzerland

AND J. ASHKENAZI

Departement de Physique de la Matière Condensée, Université de Genève, 32, Boulevard d'Yvoy, CH-1211 Genève 4, Switzerland

(*Received* 24 *January* 1980; *accepted* 21 *March* 1980)

Abstract

The electron-density distribution in Ti_2O_3 at room temperature has been determined from single-crystal X-ray diffraction data. The deformation maps show maxima of 0·15 e $Å^{-3}$ between the Ti atoms sharing a common face of O-atom octahedra, and maxima of 0·18 e $Å^{-3}$ between the O atoms and their four nearest Ti neighbours. These observations support the general view concerning the bonding in Ti_2O_3 and correlate well with the results of theoretical band-structure calculations. In particular, they confirm the existence of a metal–metal bond which is directed parallel to the ternary axis and is responsible for the anomalously low c/a ratio of this compound.

Introduction

The sesquioxides Ti_2O_3 and V_2O_3, important physically for their metal–insulator transitions, are isotypic with the corundum (α-Al_2O_3) structure but possess distinctly different structural features. The c/a ratio for Ti_2O_3 is considerably smaller than those found for most other corundum-structure oxides and may be largely attributed to the short Ti—Ti′ distance across the common face of two O-atom octahedra (Fig. 1). On the other hand, the c/a ratio for V_2O_3 is anomalously high. While maintaining the short V—V′ distance across the octahedral face, V_2O_3 is the only member of the series to have an anomalously short V′—V″ distance across an octahedral edge for such a high c/a ratio (Prewitt, Shannon, Rogers & Sleight, 1969).

The short metal–metal distances in these compounds are closely related to their electrical properties (Goodenough, 1970; Dernier, 1970; Robinson, 1974, 1975; Rice & Robinson, 1977) and are often attributed to the presence of metal–metal bonds (Goodenough, 1960, 1971, and references cited therein). In Ti_2O_3, for instance, which is insulating at room temperature, metal–metal bonds are expected to occur mainly along the c axis, *viz* across a common face of two O-atom octahedra, whereas in V_2O_3, which is metallic at room temperature, metal–metal bonds are expected to occur in a plane nearly perpendicular to the c axis, *viz* across the edges of the O-atom octahedra. These trends have also been predicted from theoretical calculations (Ashkenazi & Weger, 1976; Ashkenazi & Chuchem, 1975; Castellani, Natoli & Ranninger, 1978).

The purpose of the present study was to determine the electron-density distributions in these substances

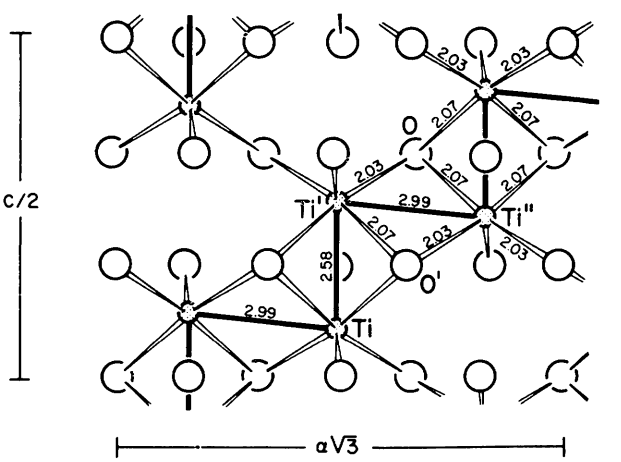

Fig. 1. A projection of the Ti_2O_3 structure on the (11$\bar{2}$0) plane. Bond lengths in Å are given to three significant figures.

* Present address: Biozentrum der Universität Basel, Klingelbergstrasse 70, CH-4056 Basel, Switzerland.

† Present address: Kristallographisches Institut der Universität Freiburg, Hebelstrasse 25, D-7800 Freiburg, Federal Republic of Germany.

0567-7394/80/050803-06$01.00

as accurately as possible and to compare them with theory. In this article we report on the deformation density of Ti_2O_3 and in the following article on that of V_2O_3 (Vincent, Yvon & Ashkenazi, 1980).

Experimental

Fragments from a large single crystal of Ti_2O_3 were spherically ground. A small specimen which appeared to be almost spherical was selected and its mean radius and e.s.d., determined from over 60 different measurements of the diameter under a high-magnification microscope, were 79 and 1 μm respectively. An analysis of intensity errors arising from non-sphericity in crystal shape (Vincent & Flack, 1979) for this crystal indicated that its deviation from sphericity was negligible and hence it could be treated as a true sphere, thus invoking the realism of applying spherical absorption corrections.

Intensities were collected with graphite-monochromated Ag $K\alpha$ radiation (λ = 0·5608 Å) in two quadrants of reciprocal space on a four-circle diffractometer in the ω–2θ scan mode out to a limit of 1·36 $Å^{-1}$ in $\sin\theta/\lambda$. The stability of the instrument was monitored by measuring three standard reflections at intervals of 100 min. Variations in the intensities were at most 1·5%. Pre-processing of the data yielded a set of intensities on a common scale with e.s.d.'s based on counting statistics, incorporating an instability term derived from the fluctuations in the standard reflections (XRAY System, 1976).

The intensities were reduced to F values corrected for the usual geometrical factors and absorption (from the A^* values of Dwiggins, 1975). However, equivalent reflections were not averaged since it had been apparent from azimuthal scans of some of the strongest reflections that anisotropic extinction effects were present in the crystal. Corrections for extinction were calculated by least squares (Becker & Coppens, 1974, 1975) with a modified version of the XRAY System's (1976) *CRYLSQ*. All data classified as observed [$I > 3\sigma(I)$] were used in the calculations with $1/\sigma^2(F)$ weights. A scale factor and atomic positional and anisotropic thermal parameters were allowed to vary simultaneously with the extinction parameters during the refinement. Scattering factors for neutral atoms were taken from Fukamachi (1971) and anomalous scattering values from *International Tables for X-ray Crystallography* (1974).

It was found that extinction could be best described as Lorentzian type I (mosaic-spread dominated) with the Thornley & Nelmes (1974) form for the angular distribution. Accurate $\bar{T}$ values, the absorption-weighted mean path lengths, were determined by the method of Flack & Vincent (1978). Of the 2073 measured reflections, 1573 contributed to sums in the refinement of 15 parameters. Convergence was reached at R = 1·6% [R_w (F) = 2·0%, S^* = 1·43]. No correlation coefficients >0·4 were obtained between the extinction parameters and the other refined parameters.

After correcting the data for extinction effects (the largest correction corresponding to a reduction in intensity of 38% for the 1120 reflection), weighted means and new e.s.d.'s were computed for equivalent reflections with weights based on the old variances. The data set reduced to 720 independent reflections of which 542 were classified as observed. Averaging of symmetry-related reflections indicated an internal consistency factor between equivalent reflections of 1·1% in intensity. This agreement suggests that multiple-reflection effects were relatively small, at least for the medium to weak reflections (Staudenmann, Coppens & Muller, 1976). However, it is not inconceivable that the anisotropic extinction-correction refinement had absorbed similar effects for the strong reflections although the smooth variations in intensities of the azimuthal scans would again indicate them to be small by comparison. A further refinement on the observed data converged at $R(F)$ = 1·3% [$R_w(F)$ = 1·0%, S = 1·73].

To establish a region of reciprocal space for which the atomic parameters were least biased by bonding effects, high-angle refinements were made at minimum $\sin\theta/\lambda$ cut-offs of 0·65, 0·7, 0·8, 0·9 and 1·0 $Å^{-1}$ (corresponding to 467, 447, 405, 351 and 290 observed reflections respectively). In all the refinements none of the positional parameters varied greatly. Indeed, the z parameter of Ti refined to exactly the same value in each case with similar e.s.d.'s. For the four lowest $\sin\theta/\lambda$ cut-off refinements, the variations on the x parameter of O were ±1 on the least significant figure – well within 1σ of the, again, similar σ's. The corresponding value for the 1·0 $Å^{-1}$ cut-off was within 1·5σ of the 0·65 $Å^{-1}$ cut-off value.

The thermal parameters and the scale factor showed greater variations among equivalent values than the positional parameters in the refinements, varying by as much as 5σ relative to the 0·65 $Å^{-1}$ cut-off refinement. The effect of correlation between the thermal parameters and the scale factor (negligibly small for the positional parameters) was adjudged to be the major cause of these variations for the following reasons. The parameters for Ti had the largest correlation coefficients with values ranging from 0·69 to 0·96 in the refinements (increasing with increasing cut-off). The parameters for O, however, were a great deal less correlated with the scale factor (<0·25) and the coefficients only became substantial (>0·5) for the 1·0 $Å^{-1}$ cut-off refinement. The influence of correlation on the observed variations was deduced from the fact that

* $S = [\sum w(F_o - F_c)^2/(NO - NV)]^{1/2}$ (NO, NV = number of observations, number of variables).

the magnitudes of the thermal parameters of O for the four lowest cut-off refinements remained within 1σ of each other.

In view of the above observations and the aims of the analyses, the atomic parameters derived from the 0·65 $Å^{-1}$ cut-off refinement were considered to be the best choice concomitant with the current data set for the calculation of deformation maps. The results of this refinement,* which converged at $R(F) = 1{\cdot}2\%$ [$R_w(F) = 1{\cdot}0\%$, $S = 1{\cdot}32$], are given in Table 1 with other relevant information.

Deformation and error maps

The deformation density at a point x,y,z, $\Delta\rho(x,y,z)$, is defined here as $\Delta\rho(x,y,z) = \rho_o(x,y,z)/k - \rho_c(x,y,z)$, where ρ_o is the Fourier transform of the unscaled observed structure factors (corrected for extinction *etc.*), k is a scale factor and ρ_c is the density calculated in the spherical-atom approximation from atomic parameters derived from high-angle X-ray data. On this basis, deformation maps were calculated in sections with the 75 observed reflections lying in the region $0{\cdot}0 < \sin\theta/\lambda < 0{\cdot}65$ $Å^{-1}$. k was determined as 2·900 (5) for this region by least squares refining on k alone (Rees & Mitschler, 1976). The inclusion of higher-order reflections did not significantly alter the bonding features but rapidly increased the noise level of the maps.

Errors in the deformation density, $\sigma(\Delta\rho)$, were estimated by the method of Rees (1976, 1978) with a modified version of his program *SIGRHO*. The errors were computed along bond axes between pairs of atoms of interest to this study, relating to the calculated sections. The contribution to the errors from the term $\sigma_{\text{model}}(k)/k$ (Rees, 1978) was estimated by calculating the scale factor for different models based on neutral and charged atoms. A value of 0·002 was obtained. The average error in ρ_o calculated from Cruickshank's (1949) formula was 0·039 e $Å^{-3}$.

* Lists of structure factors have been deposited with the British Library Lending Division as Supplementary Publication No. SUP 35173 (7 pp.). Copies may be obtained through The Executive Secretary, International Union of Crystallography, 5 Abbey Square, Chester CH1 2HU, England.

Table 1. *Crystal data for* Ti_2O_3

For brevity, only the values of the independent, refineable parameters are reported here. E.s.d.'s are given in parentheses.

Space group $R\bar{3}c$ (Hexagonal axes)		Positional and thermal parameters ‡ Ti in 12(*c*)	
a	5·1580 (4) Å†	z	0·34469 (1)
c	13·611 (1)	U_{33}	0·00403 (2)
		U_{12}	0·00196 (1)
Extinction parameters ($\times 10^{-4}$)		O in 18(*e*)	
Z_{11}	6·5 (7)	x	0·31315 (6)
Z_{22}	8·8 (6)	U_{11}	0·00468 (5)
Z_{33}	4·3 (3)	U_{33}	0·00525 (6)
Z_{12}	−4·9 (5)	U_{12}	0·00273 (3)
Z_{13}	−0·5 (6)	U_{13}	0·00065 (3)
Z_{23}	0·4 (3)	scale factor‡	2·875 (3)
μ(Ag $K\alpha$)	3·68 mm^{-1}		
μR	0·291		

† Cell parameters from Rice & Robinson (1977).
‡ Obtained from high-angle refinement (see text).

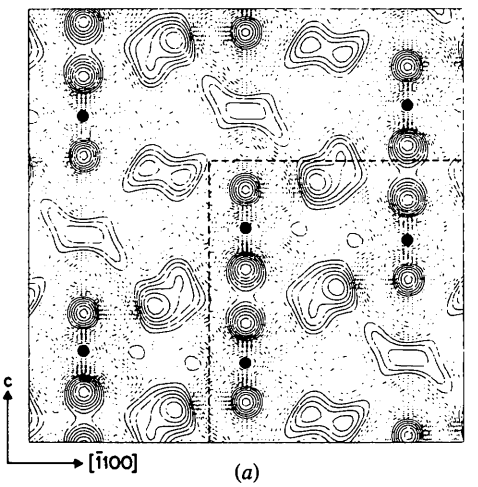

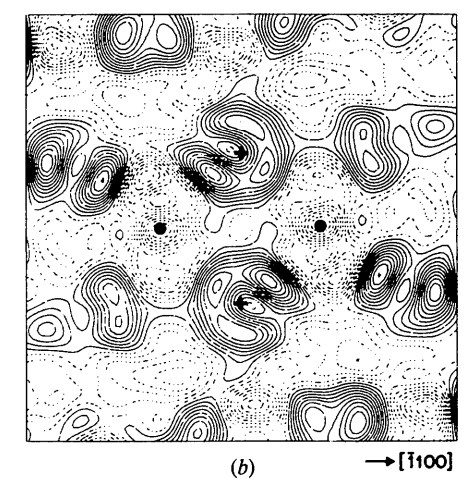

Fig. 2. (*a*) The deformation density of Ti_2O_3 in the (11$\bar{2}$0) section. The black dots indicate the Ti-atom sites represented in Fig. 1. The broken lines indicate the limits of the theoretical deformation density as shown in Fig. 4. (*b*) The deformation density of Ti_2O_3 in a section containing the O-atom sites (crosses) and Ti-atom sites (filled circles) marked O, O′, Ti′ and Ti″, respectively in Fig. 1. Contour intervals are at 0·02 e $Å^{-3}$. Negative contours are represented as dotted lines starting at 0·0 e $Å^{-3}$.

Results and discussion

Electron-density deformation maps for the two sections of major interest are shown in Fig. 2. One corresponds to the $(11\bar{2}0)$ plane containing the metal-atom sites Ti, Ti′ and Ti″, and the other to a plane containing the O-atom sites O and O′ and the metal-atom sites Ti′ and Ti″, which is tilted horizontally with respect to the $(11\bar{2}0)$ plane (Fig. 1). As can be seen from the first map there are regions of positive deformation density concentrating into ribbons of rather sharp, spherically symmetric maxima running parallel to c which are located slightly above and below the Ti-atom sites, and more diffuse non-spherically symmetric maxima lying between the columns of Ti atoms.*

Clearly, the sharp spherically symmetric maxima represent a charge deformation of the Ti atoms along the c direction which can be associated with the anticipated metal–metal bonds across the faces of the O-atom octahedra. By contrast, only little, non-significant deformation density can be found between the Ti′- and Ti″-atom sites, *i.e.* in the regions of possible metal–metal bonds across the edges of the O-atom octahedra. The deformation density and the corresponding error curves along these two directions are represented in Fig. 3. The density distribution along the Ti–Ti′ bond is not uniform but has a double-peak structure with maxima of about 0·15 e/Å^3. The error in the bonding region is of the order of 0·04 e/Å^3, whereas that on the metal-atom site is considerably higher.

The more-diffuse non-spherically symmetric maxima belong to the O atoms. Their charge deformation can be studied in the second map of Fig. 2. It shows a charge accumulation around the O- and O′-atom sites (marked by crosses) and a strong deformation of the valence-electron cloud in the directions of the nearest metal-atom sites Ti′ and Ti″ (marked by filled circles). The deformation along the two types of Ti–O bond axes is represented in Fig. 3. Clearly the features along these chemically equivalent but crystallographically non-equivalent directions are similar. In particular, the deformation-density maxima have about equal height along both Ti–O bonds and they are located at about the same distance away from the O-atom site.

From these observations one can draw two major conclusions. Firstly, a charge transfer occurs from the Ti to the O atoms. This is not unexpected and correlates with the presence of filled O p orbitals as indicated by the formal oxidation states Ti_2^{3+} O_3^{2-}. On the other hand, the deformation of the valence-electron cloud around the O atoms suggests that the Ti–O bonds are not ionic but have strong covalent character. Consequently, the net atomic charges in this compound

* The weak maxima within the ribbons of the sharp, spherically symmetric maxima are located in the centres of the empty O octahedra and are not significant.

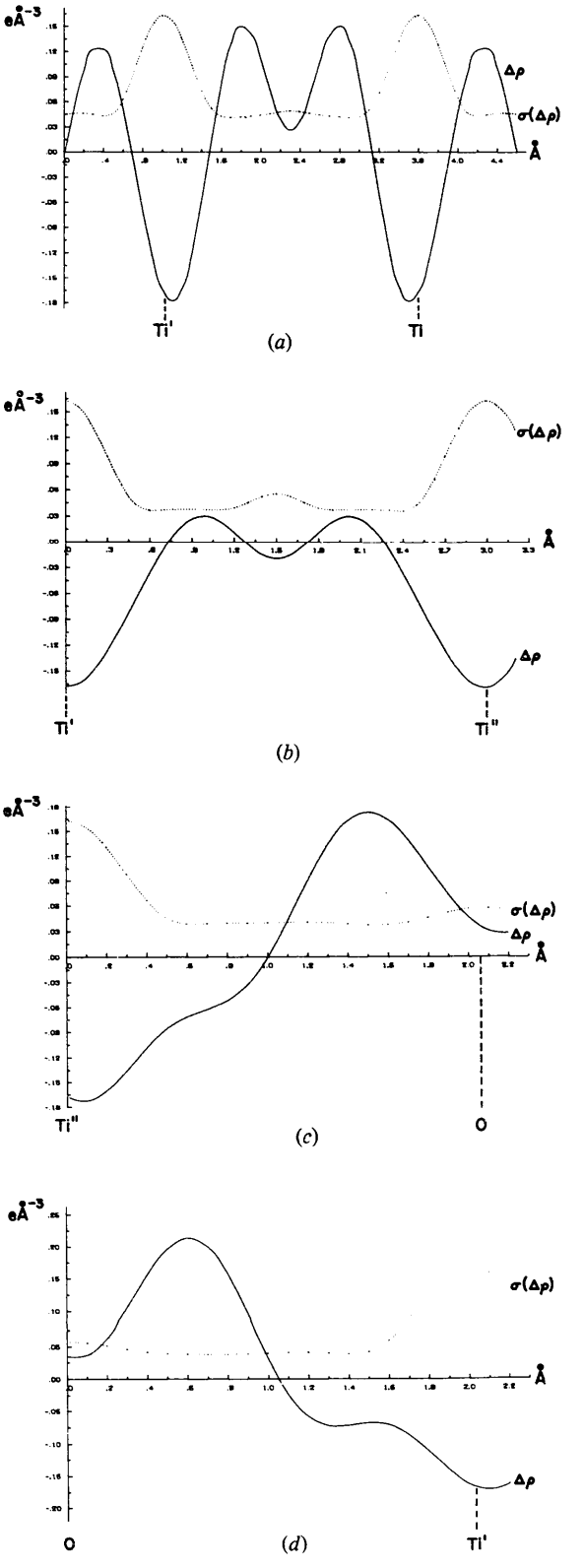

Fig. 3. The deformation density $\Delta\rho$ (solid line) and its error $\sigma(\Delta\rho)$ (dotted line) along the (*a*) Ti′–Ti, (*b*) Ti′–Ti″, (*c*) Ti″–O and (*d*) O–Ti′ vectors.

are smaller than those expressed by the above formula. No attempt has been made, however, to derive numerical values for these charges in the present work.

Secondly, the deformation density features between the Ti atoms sharing common faces of O-atom octahedra strongly support the existence of metal–metal interactions along the c direction. Since Ti^{3+} has a d^1 configuration, there are two electrons per Ti-atom pair. However, in view of the double-peak structure of the deformation density, this bond differs from that of the two-centre, two-electron bond usually found between covalently bonded atoms. The difference is probably related to the fact that the metal atoms in this compound are strongly charged and hence repel each other. This can be seen from a comparison of the Ti–O lengths given in Fig. 1. Clearly the distances between the Ti atoms and the O atoms sharing an octahedral face are longer than those between the Ti atoms and the O atoms not sharing an octahedral face. Thus the attractive interactions between the metal cations across this face are too weak to counterbalance their electrostatic repulsion. Nevertheless, they are sufficiently strong to influence the packing of the O atoms as can be seen from the c/a ratio which is anomalously low compared with that of other corundum-type oxides in which these interactions are either weak or absent.

Comparing the present electron-density maps with theory, one finds good qualitative agreement. According to a schematic band-structure proposed by Van Zandt, Honig & Goodenough (1968) and a theoretical band-structure calculated by Ashkenazi & Weger (1976), the atomic fivefold-degenerate metal $3d$ orbitals in the corundum-type oxides are split by the distorted octahedral crystal field into twofold degenerate e_g^σ and e_g^π orbitals and into a non-degenerate a_{1g} orbital. The e_g^σ orbitals are directed toward the nearest-neighbour O atoms, the e_g^π orbitals are bridging the interatomic vectors between nearest metal atoms in the basal plane and the a_{1g} orbital is directed towards the nearest metal atom along **c**. A characteristic feature of these oxides is the fact that the widths and positions of the corresponding energy bands in the crystal depend in a very sensitive manner on the metal–metal separations. In Ti_2O_3, which has an anomalously short Ti–Ti′ distance, the a_{1g} band was predicted to be split into two subbands, of which the lower one lies below the e_g^π band and is fully occupied by the two available d electrons per Ti-atom pair. Finally, the O-atom p bands were found to be filled and to show substantial d character because of mixing with the metal e_g^σ bands (Ashkenazi & Chuchem, 1975).

A theoretical deformation-density map based on these band structures is represented in Fig. 4. It shows a section of the $(11\bar{2}0)$ plane whose equivalent region in the experimental map is marked by broken lines in Fig. 2. Clearly, the features of the theoretical map are similar to those of the experimental map. In particular, the predicted d_{z^2} symmetry of the occupied a_{1g} metal-atom states as shown in the theoretical map correlates with the sharp spherically symmetric maxima located above and below the metal-atom sites. On the other hand, the weakly positive regions in the theoretical map which belong to the O-atom states are smaller than the comparable regions in the experimental map and do not show the characteristic deviation from spherical symmetry due to covalency. These discrepancies are probably due to the approximations made in the calculation of the theoretical map and will be discussed elsewhere (Ashkenazi, Vincent, Yvon & Honig, 1980).

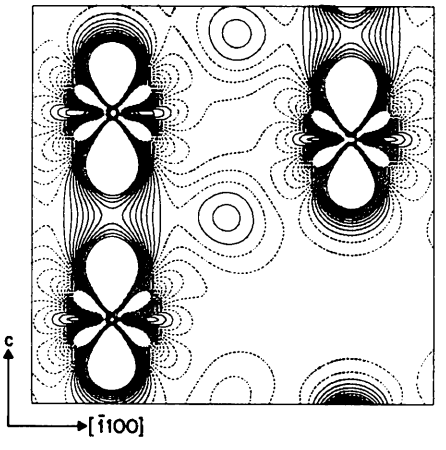

Fig. 4. Theoretical deformation density map for the metal $3d$ and oxygen $2s2p$ electrons in the $(11\bar{2}0)$ plane of Ti_2O_3, according to Ashkenazi, Vincent, Yvon & Honig (1980). Contour intervals are at 0·02 e Å^{-3}. The equivalent region in the experimental map is indicated by broken lines in Fig. 2(*a*). Negative contours are represented as dotted lines starting at 0·0 e Å^{-3}. The contours beyond ±0·22 e Å^{-3} have been suppressed.

The authors thank Professor J. M. Honig for providing the Ti_2O_3 crystal. This work was supported in part by the Swiss National Science Foundation, grant No. 2.246-0.79.

References

ASHKENAZI, J. & CHUCHEM, T. (1975). *Philos. Mag.* **32**, 763–785.

ASHKENAZI, J., VINCENT, M. G., YVON, K. & HONIG, J. M. (1980). *Solid State Commun.* In the press.

ASHKENAZI, J. & WEGER, M. (1976). *J. Phys. (Paris)*, **37**, 189–198.

BECKER, P. J. & COPPENS, P. (1974). *Acta Cryst.* A**30**, 129–153.

BECKER, P. J. & COPPENS, P. (1975). *Acta Cryst.* A**31**, 417–425.

CASTELLANI, C., NATOLI, C. R. & RANNINGER, J. (1978). *Phys. Rev. B*, **18**, 4967–5000.

CRUICKSHANK, D. W. J. (1949). *Acta Cryst.* **2**, 65–82.
DERNIER, P. D. (1970). *J. Phys. Chem. Solids*, **31**, 2569–2575.
DWIGGINS, C. W. (1975). *Acta Cryst.* A**31**, 395–396.
FLACK, H. D. & VINCENT, M. G. (1978). *Acta Cryst.* A**34**, 489–491.
FUKAMACHI, T. (1971). Tech. Rep. B12, Institute for Solid State Physics, Univ. of Tokyo.
GOODENOUGH, J. B. (1960). *Phys. Rev.* **117**, 1442–1451.
GOODENOUGH, J. B. (1970). *Proceedings of the Tenth International Conference of Physics of Semiconductors*, edited by S. D. KELLER, J. C. HENSEL & F. STERN, pp. 304–310. US Atomic Energy Commission.
GOODENOUGH, J. B. (1971). *Prog. Solid State Chem.* **5**, 145–399.
International Tables for X-ray Crystallography (1974). Vol. IV. Birmingham: Kynoch Press.
PREWITT, C. T., SHANNON, R. D., ROGERS, D. B. & SLEIGHT, A. W. (1969). *Inorg. Chem.* **8**, 1985–1993.
REES, B. (1976). *Acta Cryst.* A**32**, 483–488.
REES, B. (1978). *Acta Cryst.* A**34**, 254–256.
REES, B. & MITSCHLER, A. (1976). *J. Am. Chem. Soc.* **98**, 7918–7924.
RICE, C. E. & ROBINSON, W. R. (1977). *Acta Cryst.* B**33**, 1342–1348.
ROBINSON, W. R. (1974). *J. Solid State Chem.* **9**, 255–260.
ROBINSON, W. R. (1975). *Acta Cryst.* B**31**, 1153–1160.
STAUDENMANN, J.-L., COPPENS, P. & MÜLLER, J. (1976). *Solid State Commun.* **19**, 29–33.
THORNLEY, F. R. & NELMES, R. J. (1974). *Acta Cryst.* A**30**, 748–757.
VAN ZANDT, L. L., HONIG, J. M. & GOODENOUGH, J. B. (1968). *J. Appl. Phys.* **39**, 594–595.
VINCENT, M. G. & FLACK, H. D. (1979). *Acta Cryst.* A**35**, 78–82.
VINCENT, M. G., YVON, K. & ASHKENAZI, J. (1980). *Acta Cryst.* A**36**, 808–813.
XRAY System (1976). Tech. Rep. TR-446. Computer Science Center, Univ. of Maryland, College Park, Maryland.

Acta Cryst. (1980). A**36**, 808–813

Electron-Density Studies of Metal–Metal Bonds. II.* The Deformation Density of V_2O_3 at 295 K

BY M. G. VINCENT† AND K. YVON

Laboratoire de Cristallographie aux Rayons X, Université de Genève, 24, Quai Ernest Ansermet, CH-1211 Genève 4, Switzerland

AND J. ASHKENAZI

Departement de Physique de la Matière Condensée, Université de Genève, 32, Boulevard d'Yvoy, CH-1211 Genève 4, Switzerland

(*Received* 24 *January* 1980; *accepted* 21 *March* 1980)

Abstract

The charge-density distribution in V_2O_3 differs from that in Ti_2O_3 mainly with respect to the deformation of the metal atoms. The V atoms show a positive deformation of up to 0·1 e Å^{-3} perpendicular to **c** in a plane containing three nearest V-atom sites across the edges of the surrounding O-atom octahedra, and a negative deformation of up to 0·3 e Å^{-3} parallel to **c** between the nearest V-atom site across the faces of the O-atom octahedra. These observations are in accordance with theoretical band-structure calculations and confirm the existence of an e_π metal–metal bond which is directed across the common edges of the metal-centred O-atom octahedra.

Introduction

According to a study of the variation in the c/a ratio in corundum-type oxides (Goodenough, 1963, 1970, 1971; Prewitt, Shannon, Rogers & Sleight, 1969; McWhan, Rice & Remeika, 1969) and theoretical calculations (Ashkenazi & Weger, 1976; Ashkenazi & Chuchem, 1975; Castellani, Natoli & Ranninger, 1978), the metal–metal bonding in V_2O_3 is distinctly different from that in Ti_2O_3. Whereas the metal atoms in Ti_2O_3 interact mainly along the c direction through common faces of the O-atom octahedra, they interact in V_2O_3 mainly in directions perpendicular to the c direction through common edges of the O-atom octahedra (see metal-atom sites V, V′ and V″ in Fig. 1). In a previous article (Vincent, Yvon, Grüttner & Ashkenazi, 1980; hereafter referred to as VYGA), we have presented an experimentally determined electron-density map for Ti_2O_3 which confirms the existence of a

* Part I: Vincent, Yvon, Grüttner & Ashkenazi (1980).

† Present address: Biozentrum der Universität Basel, Klingelbergstrasse 70, CH-4056 Basel, Switzerland.

0567-7394/80/050808-06$01.00